BBA - Bioenergetics 1865 (2024) 149014

Contents lists available at ScienceDirect

BBA - Bioenergetics

journal homepage: www.elsevier.com/locate/bbabio

Anti-stokes fluorescence of phycobilisome and its complex with the orange carotenoid protein

Dmitry V. Zlenko [a,b], Elena A. Protasova [a], Georgy V. Tsoraev [a], Nikolai N. Sluchanko [c], Dmitry A. Cherepanov [d,e], Thomas Friedrich [f], Baosheng Ge [g], Song Qin [g,h], Eugene G. Maksimov [a,*], Andrew B. Rubin [a]

[a] Faculty of Biology, Lomonosov Moscow State University, Moscow 119991, Russia
[b] A.N. Severtsov Institute of Ecology and Evolution of the Russian Academy of Sciences, Moscow, Russia
[c] A.N. Bach Institute of Biochemistry, Federal Research Center of Biotechnology of the Russian Academy of Sciences, Moscow, Russia
[d] N.N. Semenov Federal Research Center for Chemical Physics, Russian Academy of Sciences, 142432 Moscow, Russia.
[e] A.N. Belozersky Institute of Physical-Chemical Biology, Moscow State University, 119991 Moscow, Russia.
[f] Technical University of Berlin, Institute of Chemistry PC 14, D-10623 Berlin, Germany
[g] China University of Petroleum (Huadong), College of Chemical Engineering, Qingdao 266580, PR China
[h] Yantai Institute of Coastal Zone Research, Chinese Academy of Sciences, Yantai 264003, PR China

ARTICLE INFO

Keywords:
Anti-Stokes fluorescence
Phycobilisomes
Photoprotection
Orange carotenoid protein
Excitation energy transfer

ABSTRACT

Phycobilisomes (PBSs) are giant water-soluble light-harvesting complexes of cyanobacteria and red algae, consisting of hundreds of phycobiliproteins precisely organized to deliver the energy of absorbed light to chlorophyll chromophores of the photosynthetic electron-transport chain. Quenching the excess of excitation energy is necessary for the photoprotection of photosynthetic apparatus. In cyanobacteria, quenching of PBS excitation is provided by the Orange Carotenoid Protein (OCP), which is activated under high light conditions. In this work, we describe parameters of anti-Stokes fluorescence of cyanobacterial PBSs in quenched and unquenched states. We compare the fluorescence readout from entire phycobilisomes and their fragments. The obtained results revealed the heterogeneity of conformations of chromophores in isolated phycobiliproteins, while such heterogeneity was not observed in the entire PBS. Under excitation by low-energy quanta, we did not detect a significant uphill energy transfer from the core to the peripheral rods of PBS, while the one from the terminal emitters to the bulk allophycocyanin chromophores is highly probable. We show that this direction of energy migration does not eliminate fluorescence quenching in the complex with OCP. Thus, long-wave excitation provides new insights into the pathways of energy conversion in the phycobilisome.

1. Introduction

Phycobilisomes (PBS) are light-harvesting complexes of cyanobacteria and red algae designed to increase the light-harvesting efficiency of photosynthetic reaction centers [1,2]. Hundreds of PBS chromophores serve as an "energy funnel" transferring excitation energy from high-energy to low-energy level chromophores delivering it to the photosystems [3] (Fig. 1). The conventional PBSs are composed of the core and six peripheral rods [3]. In *Synechocystis* sp. PCC 6803, the peripheral rods consist of three phycocyanin (PC) hexamers [4]. Each hexamer is composed of two PC trimers in a face-to-face orientation [5]. The PC trimer is composed of three αβ-heterodimers usually called "monomers". An α-subunit bears one phycocyanobilin chromophore bound to cysteine-84 residue and thus called α-84, while β-subunit bears two chromophores: β-84 and β-155 [5]. In a trimer, strong excitonic coupling of α-84 and β-84 chromophores from different monomers provides for broadening absorption spectrum by more than 10 nm [6,7]. The same effects cause shift of the α-84 and β-84 chromophores' emission maximum to 648 nm, while the β-155 chromophore emission maximum appears at 635 nm [8–10]. Certain spectral features of the chromophores can be provided by colorless linker proteins [11,12]. The PBS core is composed of three cylinders, each consisting of two allophycocyanin (APC) hexamers. Each APC-hexamer consists of two trimers composed of three αβ-heterodimers [13,14]. Both APC subunits contain one

* Corresponding author.
E-mail address: emaksimoff@yandex.ru (E.G. Maksimov).

https://doi.org/10.1016/j.bbabio.2023.149014
Received 12 May 2023; Received in revised form 6 September 2023; Accepted 18 September 2023
Available online 21 September 2023

phycocyanobilin chromophore (α-84 and β-84). The APC fluorescence has a maximum approximately at 660 nm, which gives a common notation APC660 in numerous works. Two bottom cylinders contain at least two types of red-shifted subunits: APCB (ApcD) and L_{CM} (ApcE) – the so-called terminal emitters (TE) having emission maxima at about 680 nm and composing the corresponding chromophore pool – APC680 [15,16]. The red shift of TE fluorescence facilitates the downhill transfer of excitation energy to the chlorophylls of both photosystems [17,18]. It is generally accepted that the integrity of PBS is maintained by colorless linker proteins [19]. In particular, the so-called repeating domains (REPs) of L_{CM} are essential for the PBS core integrity [20,21]. Single domain LC and LR linker polypeptides occupy the cavities of the external APC and PC trimers in the core and peripheral rods, respectively, while the two-domain linker proteins of the "rod" family maintain the structure of peripheral rods [22]. Besides the structural functions, the linker polypeptides can take part in fine tuning of the spectral properties of chromophores, as, for example, the fluorescence maximum of APC trimer shifts to 653 nm in complex with the LC linker [23]. This effect is provided by the spatial proximity and even direct contact of the LC linker globule and the chromophore.

Under excessive light conditions, the energy gathered by PBS can be dissipated into heat by the Orange Carotenoid Protein (OCP), which regulates the process of nonphotochemical quenching [24–27]. OCP is a 35-kDa water-soluble protein containing 3′-hydroxyechinenone as a chromophore and undergoing the photoconversion from an inactive (orange, OCP^O) to the active (red, OCP^R) form under blue-green light [28]. Photoactivated OCP^R delivers the ketocarotenoid to PBS and positions it at the "neck of the energy funnel," resulting in effective dissipation of the excitation energy into heat [29,30]. In several in vitro and in vivo studies, OCP was demonstrated to interact with the PBS core only, but not with the rods [31,32]. Yet, the exact location of the OCP^R binding site within the PBS core was debated for a long time [33]. However, recently it was determined by Dominguez-Martin et al. using cryo-EM technique, which revealed how the dimer of the red OCP^R form interacts with the PBS core [34]. However, the energetic coupling allowing OCP to quench the phycobilisome fluorescence effectively is still mysterious and unclear because of the relatively large distances from the PBS chromophores to the carotenoid within the PBS-bound OCP.

For a long time, two conceivable ways of how OCP^R can functionally interact with the PBS core were considered : either with APC660 [9,33,35,36] or APC680 [2,37–39]. The first hypothesis is now supported by the structural data which show that the N-domain of OCP forms a contact with the ApcA subunit located in the lower cylinder of the PBS core (see Fig. 1). Although structural data indicate that the carotenoid chromophore of OCP is slightly burrowed into the PBS, the distances from the PBS chromophores to the carotenoid within the PBS-OCP complex stay extremely large (reaching up to 27.4–35.4 Å [34]) to confidently assign the mechanism of energy transfer within the framework of known concepts. This contradiction raises questions on the effectiveness and importance of OCP as photoprotector and its ability to compete with photosystems for the energy flow from the phycobilisome pigments.

In this work, we describe the results of anti-Stokes fluorescence measurements of PBS and fragments thereof. The phenomenon of anti-Stokes fluorescence is a special case of emission when the emitted photon has more energy than the absorbed one. The background of this process was unknown and debated until 1946, when it was solved by Landau [40]. The conclusion was that only molecules in the thermally excited states can contribute to anti-Stokes fluorescence, making it significantly temperature-dependent. After identifying several unusual features of phycocyanin anti-Stokes fluorescence [41] and attributing it to the conformational mobility of the chromophores, our goal was to test this approach on the entire PBS. In this work, we show that the anti-Stokes fluorescence permits selective probing of the core PBS pigments and provides new perspectives on PBS interactions with OCP.

2. Materials and methods

2.1. OCP expression and purification

The 6× His-tagged OCP from *Synechocystis* sp. PCC 6803 with two

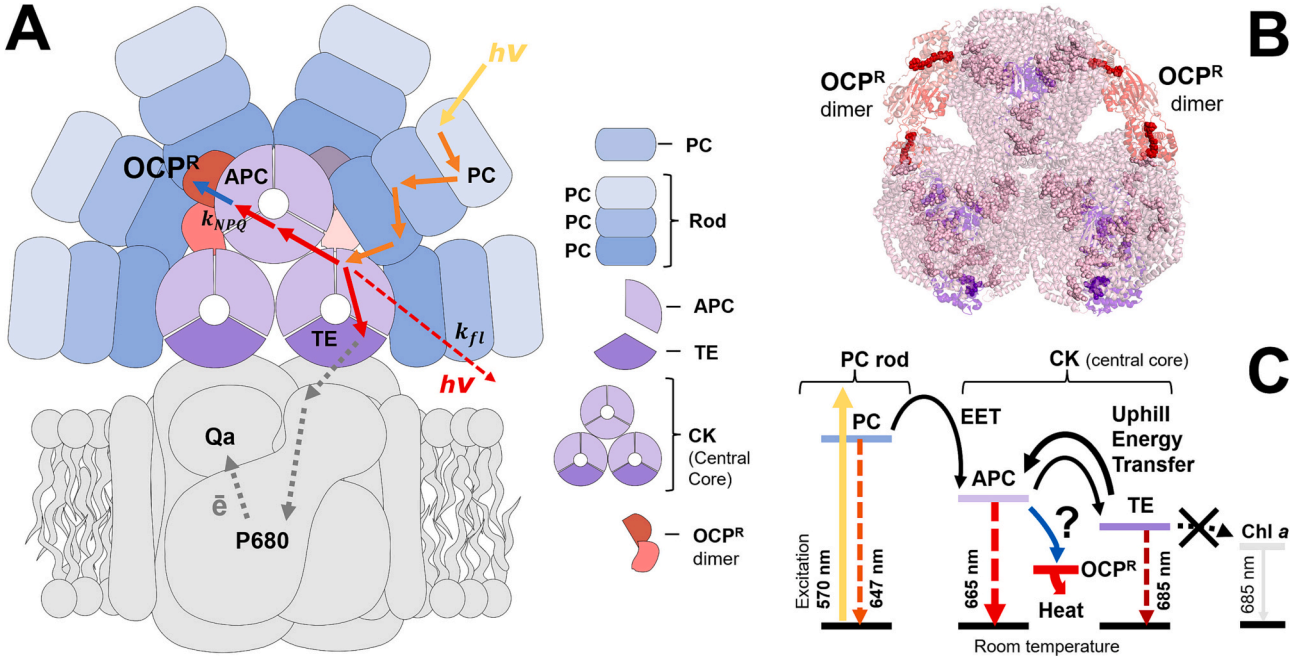

Fig. 1. A - schematic representation of the cyanobacterial phycobilisome structure and possible energy migration pathways. The OCP dimer is shown in red. The legend on the right shows the main components of the antenna complex used in this work. B - the structure of the PBS core – OCP^R complex according to the 7SC9 Protein Data Bank entry. Phycocyanin rods are not shown for clarity. Color coding according to panel A. C - ways of transformation of absorbed energy in the isolated phycobilisome presented in the form of the Jabłoński diagram.

point mutations (Y201A and W288A, OCP^{AA}) was produced in echinenone- and canthaxanthin-synthesizing *E. coli* and purified as was described earlier [42]. OCP^{AA} does not require photoactivation and is not sensitive to high phosphate content in the medium, resulting in persistent quenching of the PBS fluorescence upon mixing the samples. For these reasons, and due to structural similarities [43] this protein is used as a stable model of the active OCP^{R} state.

2.2. Native PC isolation

The C-PC sample was purified from *Arthrospira platensis* as described earlier [44]. Briefly, algae cells were harvested by centrifugation and resuspended in 20 mM phosphate buffer (pH 7.0, containing 4 mM of sodium azide), and then frozen and thawed 3 times. After subsequent centrifugation (20,000 *g* for 5 min at 4 °C, the supernatant was collected. $(NH_4)_2SO_4$ was added to a final concentration of 1.25 M and the samples were centrifuged again to obtain a crude extract of C-PC, which was then loaded onto a preequilibrated Macro-Prep Methyl hydrophobic chromatographic column. The column was then washed with phosphate buffer containing 1.25, 0.9, 0.5 and 0.2 M $(NH_4)_2SO_4$, respectively. The eluent with a purity (absorbance ratio A_{620}/A_{280}) greater than 4.0 was collected and concentrated with a 30 kDa ultrafiltration device. The buffer of the collected sample was changed to 0.6 M phosphate buffer (pH 8.0), and further purified using sucrose density gradient ultracentrifugation with a linear gradient of 0.2–0.5 M (16 h, 43,000 rpm, at 4 °C). This preparation was then lyophilized for long-term storage and transportation. Phycocyanin fractions were identified by SDS-PAGE and characteristic absorbance spectra recorded using a diode-array detector in the course of the chromatographic separation. The fractions of the main peak were collected and their SDS-PAGE indicated the presence of two bands with the apparent molecular weight of 16 and 18 kDa, corresponding to α and β C-PC chains, respectively.

2.3. APC α-subunit isolation

For the expression of *apcA* gene from *Synechocystis* sp. PCC 6803, the recombinant plasmid pCDFDuet-apcA-cpcEF-ho1-pcyA was co-expressed in *E. coli* BL21 (DE3) according to the protocols described earlier [45–47]. The recombinant ApcA was then purified by metal affinity and size-exclusion chromatography.

2.4. Isolation of phycobilisomes

PBSs were isolated from wild-type *Synechocystis* sp. PCC 6803 cells as described earlier [37]. The CK mutant of *Synechocystis* sp. PCC 6803 [4] lacking phycocyanin, i.e. lacking peripheral rods of PBS, was used to isolate the PBS cores. The ΔPBLCM mutant of *Synechocystis* sp. PCC 6803 [48], lacking conventional PBSs, was used as a source of pure phycocyanin resembling the PBS peripheral rods [12]. Cyanobacterial cells were pelleted by centrifugation (7000 rpm for 15 min) and washed twice with 0.75 M PBS buffer (pH 7.6). The cells were sonicated (160 cycles, 5 s sonication periods with 5 s gaps between them) in the 0.75 M phosphate buffer supplemented with Triton X-100 (2 % *v*/v) and incubated for 40 min at room temperature. Then, the debris was removed by centrifugation (15,000 rpm for 30 min). The supernatant was loaded onto a linear (0.25–1.25 M) sucrose density gradient in 0.75 M phosphate (pH 7.6) for ultracentrifugation at 170,000 *g* for 3 h (41,000 rpm, Beckman 70 Ti rotor, 20 °C). After centrifugation, the material was collected from the bottom of each tube using a thin needle and a roller pump. The sucrose concentrations were measured using a PZO RR 11 manual refractometer (PZO, Warsaw, Poland) for each fraction. The phycobilisome integrity was verified by measuring fluorescence spectra at 77 K. At 570 nm excitation, the spectrum of intact phycobilisomes is characterized by a minor contribution of any states except 685 nm, corresponding to the fluorescence of terminal emitters (data not shown), which proves the high efficiency of energy transfer from the phycocyanin to the core and, consequently, the integrity of the phycobilisome.

2.5. Time-resolved fluorescence measurements

Fluorescence decay kinetics were obtained using a time-correlated single photon counting (TCSPC) detector with an ultra-low dark count rate (HPM100-07C, Becker&Hickl, Germany), and an ML-44 monochromator (Solar LS, Minsk, Belarus) used for tuning the detection wavelength from 600 to 750 nm in 5 nm steps. The fluorescence spectra were recorded using a 1 nm step. Regular Stokes fluorescence was excited at 570 nm (repetition rate 80 MHz, pulse width 150 fs, average optical power 3.2 mW) using the second harmonics of a femtosecond optical parametric oscillator (TOPOL-1050-C, Avesta Project LTD, Russia) pumped by a femtosecond Yb-laser (TEMA-150, Avesta Project LTD). Anti-Stokes fluorescence was excited at 770 nm (repetition rate 80 MHz, pulse width 150 fs, optical power 685 mW) using the signal output wavelength of the same femtosecond optical parametric oscillator. The laser beam was defocused on the sample to a diameter of about 6 mm to avoid two-photon excitation. The resulting photon fluxes were about 0.2 and 32 μmol quanta m^{-2} s^{-1} for 570 and 770 nm excitation, respectively. The TCSPC time unit is 50 ns, which can be reduced by a gain function up to 15 times, which, taking into account the maximum number of time channels (4096), provides photon recording in short steps from 12.2 down to 0.813 ps. Considering the frequency of our fs generator (80 Hz), the corresponding detection interval was chosen with the gain equal to 4, which corresponds to 12.5 ns. For conventional fluorescence, we used 4096 time channels, which gives a time step of 3.05 ps. For IR excitation experiments, we chose 1024 time channels (a time step of 12.2 ps) to compensate for the much lower fluorescence intensity level and to reduce the signal accumulation time.

The emission signal was collected perpendicular to the excitation beam. To avoid the detection of scattered laser beam, the following edgepass filters (Thorlabs, USA) were utilized: a longpass 600 nm filter for Stokes fluorescence and a shortpass 750 nm filter for Anti-Stokes fluorescence. The temperature of the samples was stabilized at 35 °C by a cuvette holder Qpod 2e with a magnetic stirrer (Quantum Northwest, USA). The temperature dependence measurement of Anti-Stokes fluorescence was investigated in the range from 5 to 60 °C with 5 °C steps. All proteins were dissolved in phosphate buffer (0.75 M sodium phosphate, pH 7.6), which is necessary for the integrity of PBS and its core [49].

Global analysis fitting was performed for the time-resolved fluorescence spectra using the Matlab (USA) software. With global analysis, all wavelengths were analyzed simultaneously with a set of common time constants. An experimentally measured instrumental response function (IRF) was used to approximate the fluorescence decay kinetics and to determine the characteristic lifetimes. For this purpose, we recorded the attenuated signal from the laser as scattering in water. The kinetic parameters were found by numeric nonlinear minimization of the solution to fit the experimental data in the spectral interval of 600–750 nm and the time range of 10 ps – 12.5 ns.

In the global analysis, the spectro-temporal matrix $\Delta A(\lambda, t)$ is decomposed in terms of a linear combination of n discrete exponential functions $P_i(t) = exp(-t/\tau_i)$:

$$Q[\tau](t,\lambda) = \sum_{i=1}^{n} D_i(\lambda) \cdot P_i(t-t') \otimes IRF(t') \quad (1)$$

Here $P_i(t-t') \otimes IRF(t')$ denotes the standard convolution equation:

$$P_i(t-t') \otimes IRF(t') = \int_0^t IRF(t') \cdot exp\left(-\frac{t-t'}{\tau_i}\right) dt' \quad (2)$$

We used the assumption, based on the general solution of a system of linear coupled first-order differential equations, that the lifetimes, $\tau = \{\tau_i\}$, are independent of the emission wavelength λ and hence can be treated as "global" fit parameters. The wavelength-dependent pre-

exponential amplitudes $D_i(\lambda)$ associated with each lifetime τ_i define the Decay-Associated Spectra (DAS). For each set of lifetimes $\{\tau_i\}$, the spectral amplitudes $D_i(\lambda)$ can be found by solving the Linear Least Squares Regression (LLSR) problem following the standard methods of data regression [50]. The optimum values of τ are obtained by nonlinear minimization of the normalized sum of squared residuals

$$R[\tau] = (L \cdot M - n)^{-1} \sum_{l=1}^{L} \sum_{m=1}^{M} [\Delta A(\lambda_l, t_m) - Q[\tau](\lambda_l, t_m)]^2 \quad (3)$$

The post-processing and visualization of calculated data were performed using the Origin Pro 2018 package (OriginLab Corp., USA).

All experiments were repeated at least three times on different protein preparations.

3. Results and discussion

When the PBS was excited at 570 nm, we observed a well-known pattern of evolution of the time-resolved spectra (Fig. 2A). The position of the fluorescence maximum gradually shifted to the red region, which is known to reflect the transfer of electronic excitation energy from the phycocyanin chromophores in the rods to the chromophores of the phycobilisome core. To analyze changes in the fluorescence spectra, we applied a global analysis, which allowed us to present the kinetic data in the form of Decay-Associated Spectra (DAS). For clarity, we do not show components with time constants of less than 40 ps. These may be associated with fast energy transfer processes between neighboring chromophores, but, given the temporal resolution of our setup (instrumental response function (IRF) is shown in Figs. 1F and 5F, FWHM = 37 ps), we refrain from interpretation of these ambiguous signals. Nevertheless, we can confidently attribute the 100 ps component to the energy transfer from the rods to the PBS core due to the characteristic shape of the DAS, which has a negative amplitude in the 670–680 nm region. To our surprise, the differences between Stokes and anti-Stokes PBS fluorescence (Fig. 1B) appeared in the absence of energy transfer from the rods to the core. Indeed, at 770 nm excitation, we observed a minor DAS contribution with a time constant of about 120 ps with a positive amplitude in the 660–680 nm region and a negative amplitude in the 640 nm region (Fig. 1D), which can probably be interpreted as an uphill energy transfer from the core to the rods. On top of this, we observed a major component with a lifetime of 1.4 ns and a maximum at 670 nm under short-wave and long-wave excitation, which can be attributed to the fluorescence of allophycocyanin chromophores in the PBS core, including terminal emitters. Thus, we can conclude that PC rod fluorescence is excited to a significantly diminished level when the PBS is excited in the near-infrared region. As a result, the steady-state anti-Stokes fluorescence spectrum of PBS is slightly narrower compared to the conventional spectrum (Fig. 1E) due to the absence of the contribution of low-quantum yield PCs involved in energy transfer. The second important observation is the direct excitation of the core chromophores using infrared quanta, as evidenced by the faster rise in the fluorescence signal in the kinetics at 680 nm (Fig. 1F).

Even looking at the time-resolved spectra (Fig. 1A and B) with the naked eye, it is obvious that the PBS fluorescence signal looks much simpler when excited in the IR. Thus, this mode of optical excitation

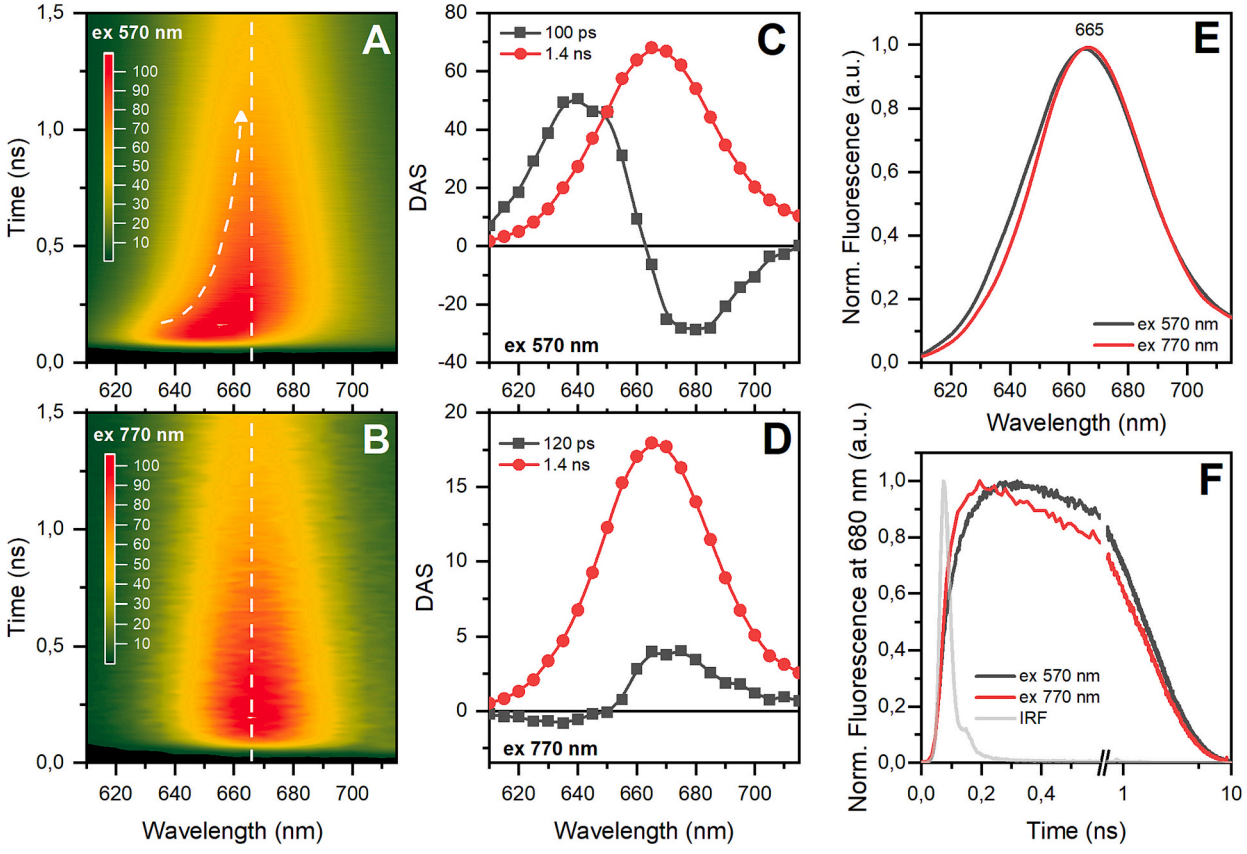

Fig. 2. Time-resolved Stokes (A) and anti-Stokes (B) fluorescence spectra of isolated PBS in 0.75 M phosphate buffer excited by 150 fs laser pulses at 570 and 770 nm, respectively. The fluorescence intensity is shown in color, the linear color scale is shown in each panel. Decay-associated spectra (DAS) of PBS fluorescence in the Stokes (C) and anti-Stokes (D) regimes. The numbers indicate characteristic kinetic components derived from the global analysis of time-resolved fluorescence spectra measured in the range from 600 to 750 nm. (E) – normalized steady-state Stokes (black) and anti-Stokes (red) fluorescence of PBS. (F) – fluorescence decay kinetics of PBS at 680 nm excited by 150 fs laser pulses at 570 (black) and 770 nm (red). Note the break of timescale at 0.6–0.7 ns introduced for better presentation of fluorescence rise kinetics. The instrumental response function (IRF) is shown in gray. Time zero is shifted from the IRF intensity maximum by 2 FWHM for better presentation. The temperature of the samples was stabilized at 35 °C during all experiments.

makes it possible to selectively probe the PBS core pigments and eliminate hundreds of rod chromophores involved in the entangled chain of energy transfer from consideration. However, in order to focus on the excitation energy conversion processes of interest in the interactions of PBS with OCP, we need to ensure that we interpret the kinetic data correctly and do not confuse the energy migration processes between PBS chromophores and the conformational dynamics of the chromophores. As we showed earlier, the conformational mobility of phycocyanin chromophores can be due to spontaneous changes in its oligomeric state [41]. On the other hand, recent work has demonstrated, using structural methods [34], that the PC rods of PBS are able to move, which probably can also affect the local environment of the chromophores and lead to changes in their lifetimes. In order to answer this question, we decided to conduct additional experiments and investigate the anti-Stokes fluorescence of the main building blocks of PBS.

A comparison of the characteristics of Stokes and anti-Stokes fluorescence of PBS components is shown in Fig. 3. The left column shows the stationary spectra (Fig. 3A, B, C, and D), and to the right of these panels are the results of the global analysis of the corresponding time-resolved spectra (Fig. 3E-L). The seemingly simple case of the recombinant allophycocyanin α-subunit (ApcA) with a single chromophore bound to the protein clearly demonstrates the differences between the Stokes and anti-Stokes fluorescence of this class of fluorophores. The

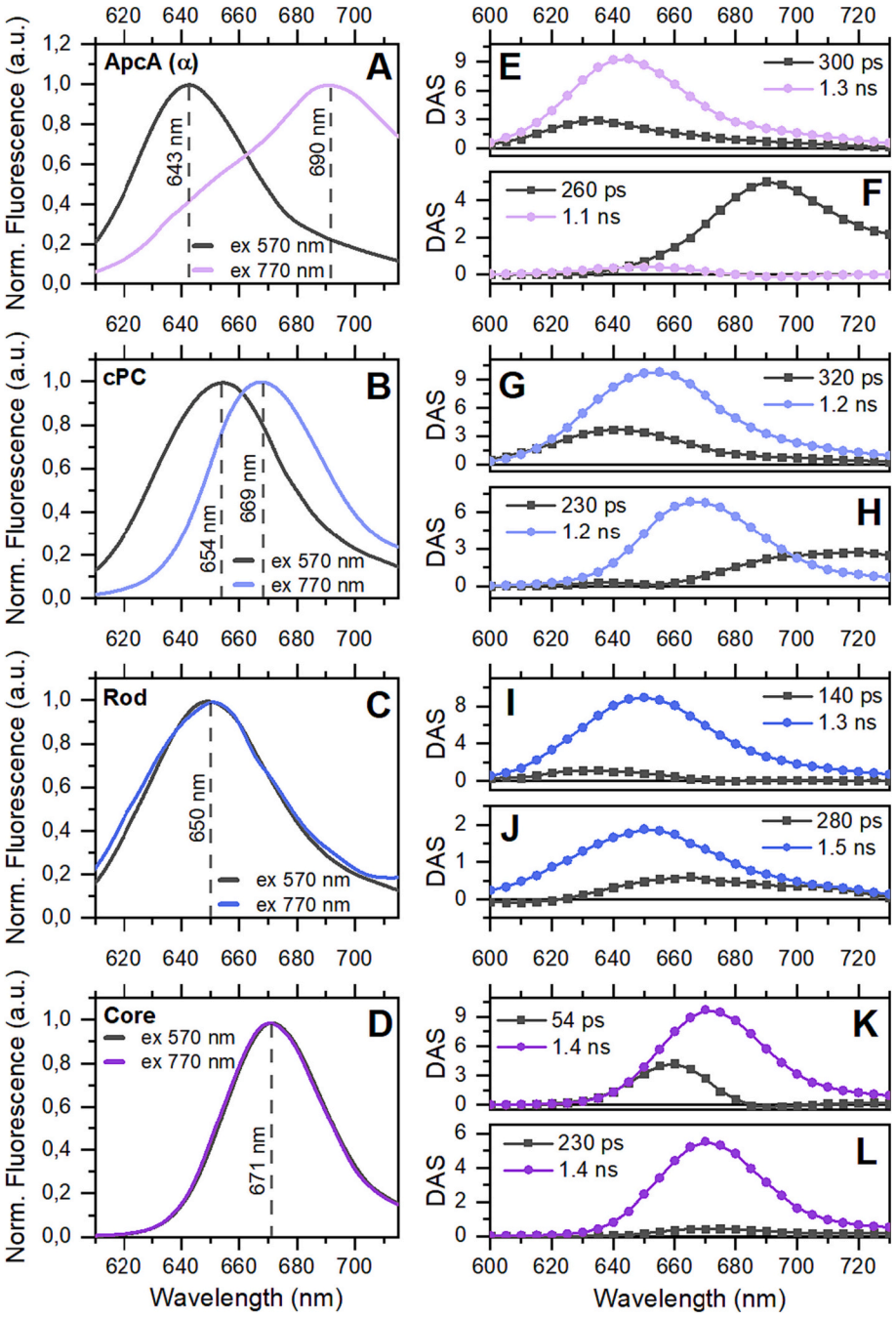

Fig. 3. Steady-state Stokes (black lines) and anti-Stokes (colored lines) fluorescence spectra of monomeric α-subunit of APC (A), trimeric cPC (B), PBS rods (C) and PBS cores in 0.75 M phosphate buffer registered upon 570 and 770 nm excitation. Time-resolved spectra were recorded with a 150 fs laser pulse excitation at 35 °C. To the right of the steady-state spectra, panels display the corresponding Decay-associated spectra (DAS) in the Stokes (E, G, I and K) and anti-Stokes (F, H, J and L) regimes. The numbers indicate characteristic kinetic components derived from the global analysis of time-resolved fluorescence spectra.

observed variations in the position of the fluorescence maximum with respect to changes in the excitation mode of ApcA (Fig. 3A, E and F) are likely related to the conformational mobility and, consequently, the heterogeneity of the chromophore and also strongly resemble the properties of phycocyanin that we described in detail earlier [41]. The nature of these changes is related to the disruption of the planarity of the chromophore, as a result of which the absorption spectrum is significantly shifted to the red region, and the lifetime of the excited state is reduced to several hundred picoseconds.

We would like to note that in the case of ApcA, the differences between the Stokes and anti-Stokes fluorescence spectra are greater compared to PC, most probably because PC chromophores are stabilized due to protein-protein contacts between the α- and β-subunits within the cPC trimer, whereas such contacts are absent in ApcA monomeric α-subunits. In the spectra of ApcA anti-Stokes fluorescence, a component with a nanosecond lifetime is almost completely absent, although the fast component also appears in the normal mode, its maximum position differs by almost 60 nm (Fig. 3E and F), indicating significant heterogeneity in the electronic levels of the chromophores in a non-rigid protein environment. Here we would like to remind our readers of the hypothesis about the interaction of OCP and PBS due to the direct contact of OCP's keto-carotenoid and some bilin of the PBS. This possibility was discussed for the first time after experiments with cross-linked proteins [51], which indicated that the N-domain of OCP is burrowed between ApcA and ApcE. More recent structural data do not reject the possibility of direct contact of the chromophores, showing that the distances between the chromophores are quite small [34]. We would like to note that if a carotenoid is indeed able to influence the configuration of the chromophore, the latter can potentially turn into a trap for excitation of neighboring core pigments. However, the possibility of such conformational rearrangements has yet to be proven.

In the case of recombinant proteins or purified preparations of phycobiliproteins, the increased conformational mobility of chromophores is not surprising, since such proteins lack the colorless linker proteins that stabilize the antenna complex and are responsible for the fine-tuning of the spectral characteristics of chromophores. Indeed, in the case of PC rods, we see a much smaller contribution of states with short lifetimes (140–280 ps) in both the Stokes and anti-Stokes modes (Fig. 3 C, I, and J). This is probably the reason for the significant similarity of the steady-state fluorescence spectra (Fig. 3C). In the case of PBS cores, we also observe significant similarities between the stationary spectra of Stokes and anti-Stokes fluorescence (Fig. 3D), as well as an almost complete absence of the contribution of fast components in the fluorescence decay kinetics (Fig. 3K and L). Moreover, in terms of the model for describing the fluorescence decay kinetics, the PBS core represents the simplest case and can be adequately approximated by a monoexponential decay. Thus, we conclude that in high-quality PBS preparations the fast components of the anti-Stokes fluorescence spectra represent a minor fraction and are probably not related to spontaneous chromophore isomerization, since such conformational changes are hampered by stabilizing factors such as linker proteins and other protein-protein contacts. We believe that anti-Stokes fluorescence can be a test for the quality of PBS preparations, because in case of disruption of PBS integrity and/or contamination by individual PBS fragments, the fluorescence spectrum will change significantly through the shifts of the emission maximum.

For the subsequent assignment of the anti-stokes PBS fluorescence and determination of the contributions of the core and rods to the total signal, we performed additional experiments. As shown in our previous work [2], the absorption spectrum of the complete PBS can be represented as the arithmetic sum of the absorption of the core and rods (Fig. 4A). Decomposition of the PBS absorption spectrum into its components makes it possible to estimate the ratio of the optical densities of the core and rods at a given wavelength. Our estimates show that at 570

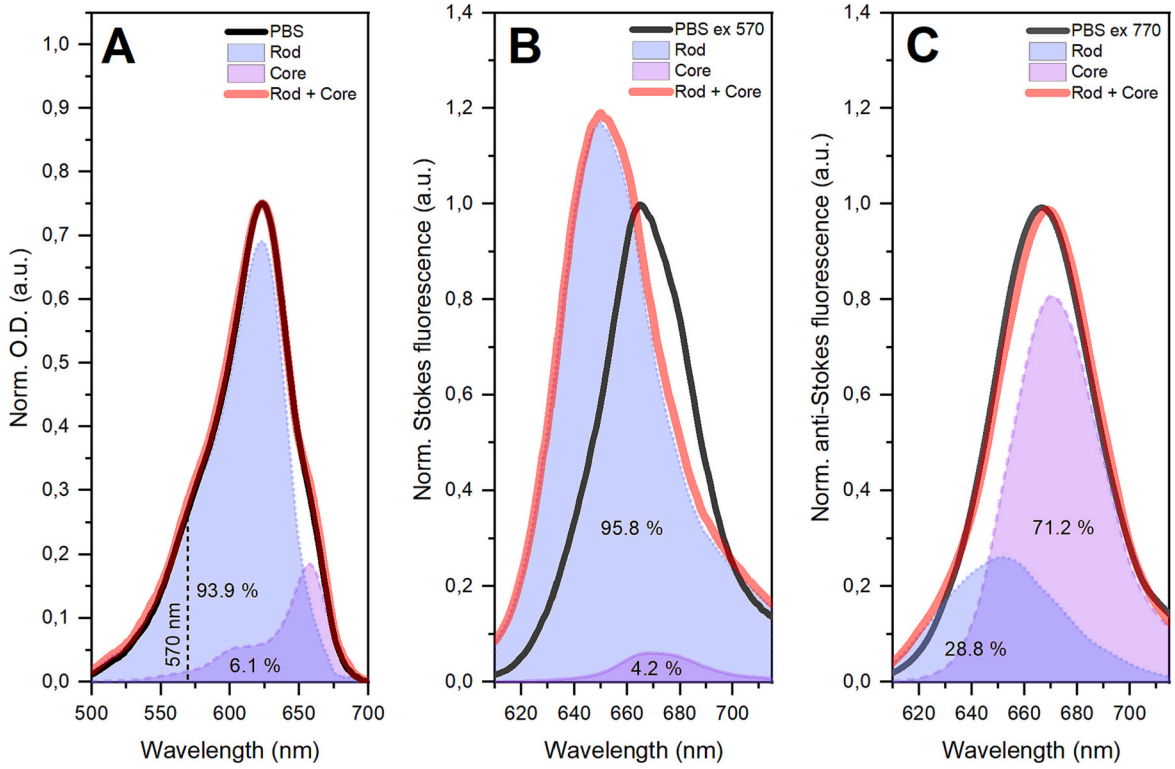

Fig. 4. (A) - decomposition of PBS absorbance spectrum (black line). Red line represents the sum of contributions from PC rods (cylindrical PBS from ΔPB-domain mutant, blue area) and PBS cores (PBS from the CK mutant lacking PC, purple area). Numbers indicate the contribution of rods and cores to PBS absorption at 570 nm. (B) - fluorescence yield of intact PBS, rods, and cores taken in the proportions shown in panel A at 570 nm excitation. The red line represents the sum of PC rods and PBS cores emission. PBS fluorescence spectrum is normalized to 1 at the maximum intensity. (C) - fluorescence yield of intact PBS, rods, and cores taken in the proportions shown in panel A at 770 nm excitation.

nm almost 94 % of the energy is absorbed by the rods due to the large number of chromophores in these parts of the antenna, as well as a shift in the absorption of the core into the red region. However, the accuracy of optical density measurements is insufficient to estimate such ratios at 770 nm, so we applied an alternative approach by measuring and comparing the fluorescence yields of PBS fragments. For this approach, we took specific concentrations of cores and rods corresponding to their absorption within the PBS (Fig. 4A) and compared their fluorescence spectra with the fluorescence spectrum of the whole PBS. We found that under excitation at 570 nm in the absence of the core, the fluorescence yield of the rods is significantly higher, which is obviously due to the absence of transfer of electronic excitation energy to the core pigments (Fig. 4B). Under the same conditions, the core fluorescence yield is extremely low due to the low extinction at 570 nm. At the same time, the relative fluorescence intensity of the rods is about 96 %, which corresponds well to the ratio of the optical densities of the rods and the core at 570 nm (Fig. 4A) and can be easily explained by comparable fluorescence quantum yields of major chromophore populations.

Obviously, at 570 nm excitation, the PBS fluorescence spectrum is not a simple arithmetic sum of the rod and core fluorescence spectra because of the energetic coupling. However, at 770 nm excitation, we found that the situation is the opposite. In this case, we observe a significantly greater emission from the core fluorescence, and the sum of the spectra of the core and rods matches closely the intensity and shape of the fluorescence spectrum of the whole PBS (Fig. 4C). This observation, first, shows that the core chromophores absorb significantly better at 770 nm. Assuming that the quantum yields of the major states of the core and rods are equal (since their lifetimes are almost identical), we can estimate the ratio of core and rod extinction coefficients as 2.5 to 1 at 770 nm. And second, it proves that at 770 nm the core and rods are excited directly and independently of each other, while energy interactions appear to be insignificant.

Next, we proceed to the description of the energetic interactions of the PBS and OCP, which for clarity is presented in Fig. 5 in a similar way as in Fig. 2. Analysis of the instantaneous PBS fluorescence excited at 570 nm (Fig. 5A) shows that, during the formation of the PBS complex with OCP in the active state, energy transfer from the rods to the core does not stop, but the contribution of the previously dominant state with a lifetime of about 1.4 ns is significantly reduced (Fig. 5C), essentially being replaced by a state with a lifetime of about 180 ps. When PBS-OCP^{AA} complexes are excited in the near IR range, we observe no energy transfer from the rods to the core, nor any signal from the rods at all. The major component obviously corresponds to quenched allophycocyanin chromophores of the PBS core. Thus, when excitation is performed at 770 nm, we directly excite the core pigments, which are then quenched by energy transfer to the carotenoid in OCP. Given the fact that the maximum position of the minor component is shifted relative to the bulk APC peak (665 nm) into the red region by about 10 nm (to 675 nm), we can attribute this signal to terminal emitters (ApcE and others). We found no traces of energy transfer from red pigments to blue pigments within the PBS core, probably because this process may occur rapidly enough to be beyond the capabilities of our registration system; however, the increased lifetime of bulk APC indicates that it may be excited indirectly after absorption of terminal emitters. It should be noted that

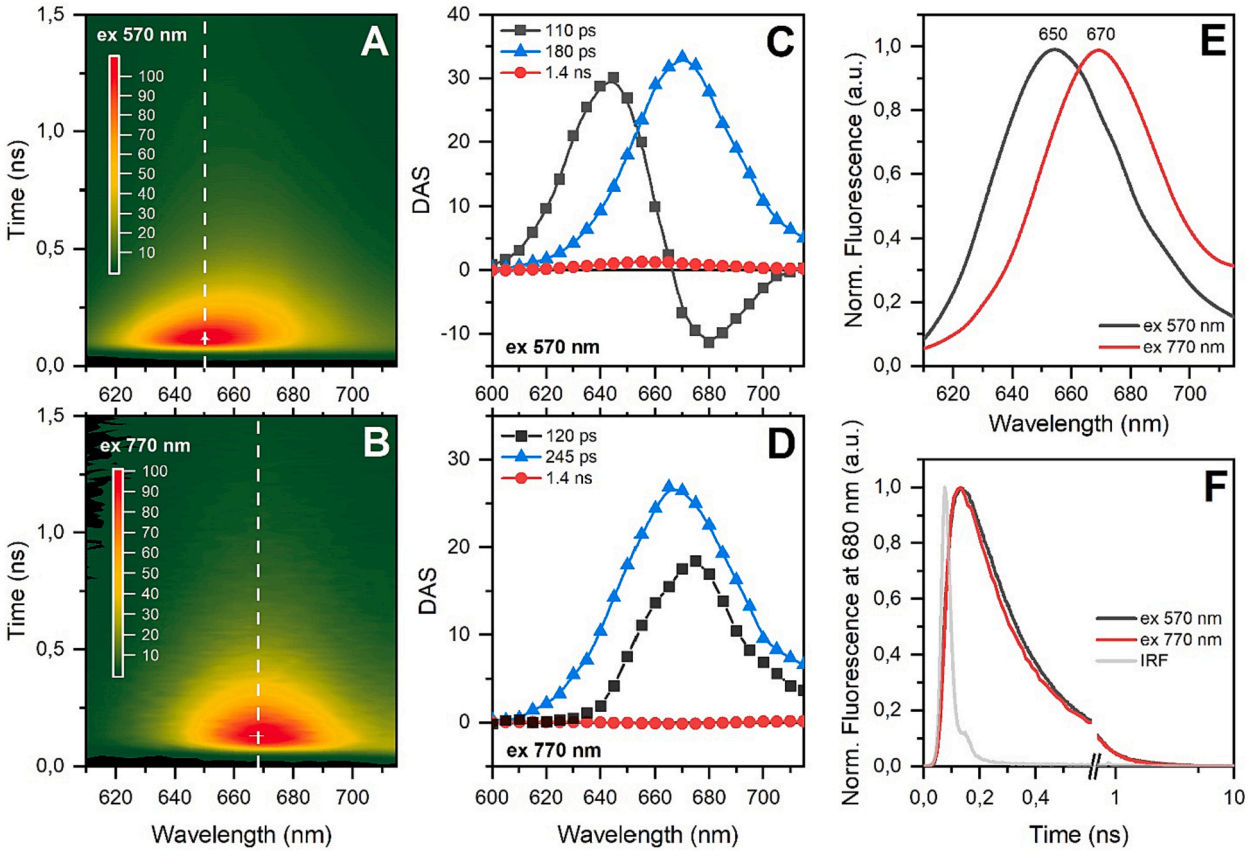

Fig. 5. Effect of OCP-induced quenching on the time-resolved Stokes (A) and anti-Stokes (B) fluorescence spectra of isolated PBS-OCP^{AA} complexes in 0.75 M phosphate buffer excited by 150 fs laser pulses at 570 and 770 nm, respectively. The fluorescence intensity is shown in color, the linear color scale is shown in each panel. Decay-associated spectra (DAS) of PBS fluorescence in the Stokes (C) and anti-Stokes (D) regimes. The numbers indicate characteristic kinetic components derived from the global analysis of time-resolved fluorescence spectra measured in the range from 600 to 750 nm. (E) – normalized steady-state Stokes (black) and anti-Stokes (red) fluorescence of PBS. (F) – fluorescence decay kinetics of PBS at 680 nm excited by 150 fs laser pulses at 570 (black) and 770 nm (red). Note the break of timescale at 0.6–0.7 ns introduced for better presentation of fluorescence rise kinetics. The instrumental response function (IRF) is shown in gray. Time zero is shifted from the IRF intensity maximum by 2 FWHM for better presentation. The temperature of the samples was stabilized at 35 °C during all experiments.

in the case of regular excitation (570 nm), the fluorescence of terminal emitters is masked by energy transfer (see Fig. 5C).

It may seem surprising that the lifetime of quenched APC chromophores is about 120–250 ps, but it is worth recalling that there are about 60 pigments in the core, so probably the rather slow relaxation of excited states is due to delocalization of excitation between pigments with similar spectral characteristics. Undoubtedly, the anti-Stokes fluorescence excitation mode allows us to greatly simplify the kinetic scheme of the energy conversion processes in the PBS (Fig. 5D). The absence of the contribution of rod chromophores to the spectra and kinetics allows the events in the phycobilisome core to be observed without the need to take into account the energy transfer steps, which occur at comparable rates with the OCP-induced non-photochemical quenching. Thus, we believe that anti-Stokes fluorescence can provide valuable insights into the mechanisms of energy conversion in photosynthetic light-harvesting complexes.

4. Conclusions

Near coincidence of the shapes of the long-living components of the Stokes and anti-Stokes DAS of the entire unquenched PBS (Fig. 2) demonstrates the effectiveness of the PBS functioning. Despite the type of chromophore predominantly absorbing light, the emission occurs from the PBS core. Indeed, at 570 nm excitation, about 93 % of the energy is collected by PC rods, while at 770 nm, 71 % is collected by the core pigments; thus, the long-living DAS components coincide as well as the steady-state spectra. Thus, the use of low-energy excitation allows us to selectively excite the chromophores in the PBS core without engaging the rod pigments, which greatly simplifies the scheme of energy transfer processes in the PBS.

We showed that the mobility of the phycobiliprotein chromophore is maximized when there is a lack of stabilizing protein-protein contacts from neighboring pigment-protein complexes and/or colorless linkers. Given the conformational mobility of the phycobilisome structure [34] and chromophores within the phycobiliproteins [41], the shift of the anti-Stokes fluorescence maximum in the spectrum of the OCP-quenched PBS samples (Figs. 2E and 5E) and corresponding DAS components (Figs. 2D and 5D) can be treated in two ways. First of all, one can state that OCP destabilizes the PBS structure and, therefore, provides for the appearance of some red-shifted chromophore subpopulations. Taking into account recent results showing that the phycobilisome can switch between several conformational states during the transition from the light-harvesting state to the photoprotective state by the movement of phycocyanin cylinders [34], this hypothesis may be valid. Another possibility is that the integrity of the PBS was disrupted by OCP, but this option seems unlikely because even in the detached rods the contribution of long-wavelength fluorescence remained minimal.

The observed increase in the decay time constants under 770 nm excitation of the PBS-OCP complex (Fig. 5) implies, in particular, a prolongation of the energy transfer pathway from the chromophore that collected light to the special pigment that interacts with the carotenoid in OCP. Excitation of terminal emitters (see Fig. 1) can contribute for the increase in the decay time of bulk APC chromophores, as the rate and efficiency of the uphill energy transfer will always be lower than the ones of the downhill transfer.

Finally, we believe that the anti-Stokes fluorescence signatures demonstrated in this work may be useful for studying the integrity of the phycobilisome, its conformational mobility, and clarifying the mechanism of OCP-dependent non-photochemical quenching.

Declaration of competing interest

The authors declare that they have no known competing financial interests or personal relationships that could have appeared to influence the work reported in this paper.

Data availability

Data will be made available on request.

Acknowledgments

Authors are grateful to Yury Slonimskiy for help with OCP^{AA} expression, isolation, and purification.

Spectroscopic experiments and all experiments with the phycobilisomes were supported by the Russian Science Foundation (grant number 21-44-00005); and the National Natural Science Foundation of China (grant number 42061134020). OCP^{AA} purification and analysis were supported by the the Ministry of Science and Higher education of the Russian Federation in the framework of the Agreement no. 075-15-2021-1354 (07.10.2021).

Appendix A. Supplementary data

Supplementary data to this article can be found online at https://doi.org/10.1016/j.bbabio.2023.149014.

References

[1] E.G. Maksimov, F.I. Kuzminov, I.V. Konyuhov, I.V. Elanskaya, V.Z. Paschenko, Photosystem 2 effective fluorescence cross-section of cyanobacterium Synechocystis sp. PCC6803 and its mutants, J. Photochem. Photobiol. B Biol. 104 (2011) 285–291.
[2] E.A. Protasova, T.K. Antal, D.V. Zlenko, I.V. Elanskaya, E.P. Lukashev, T. Friedrich, K.S. Mironov, N.N. Sluchanko, B. Ge, S. Qin, E.G. Maksimov, State of the phycobilisome determines effective absorption cross-section of Photosystem II in Synechocystis sp. PCC 6803, Biochim. Biophys. Acta 2021 (1862) 148494.
[3] N. Adir, Elucidation of the molecular structures of components of the phycobilisome: reconstructing a giant, Photosynth. Res. 85 (2005) 15–32.
[4] A.A. Arteni, G. Ajlani, E.J. Boekema, Structural organisation of phycobilisomes from Synechocystis sp. strain PCC6803 and their interaction with the membrane, Biochim. Biophys. Acta 2009 (1787) 272–279.
[5] P.-P. Peng, L.-L. Dong, Y.-F. Sun, X.-L. Zeng, W.-L. Ding, H. Scheer, X. Yang, K.-H. Zhao, The structure of allophycocyanin B from Synechocystis PCC 6803 reveals the structural basis for the extreme redshift of the terminal emitter in phycobilisomes, Acta Crystallogr. Sect. D 70 (2014) 2558–2569.
[6] M. Gwizdala, T.P.J. Krüger, M. Wahadoszamen, J.M. Gruber, R. van Grondelle, Phycocyanin: one complex, two states, two functions, J. Phys. Chem. Lett. 9 (2018) 1365–1371.
[7] K. Sauer, H. Scheer, Excitation transfer in C-phycocyanin. Förster transfer rate and exciton calculations based on new crystal structure data for C-phycocyanins from *Agmenellum quadruplicatum* and *Mastigocladus laminosus*, Biochim. Biophys. Acta 936 (1988) 157–170.
[8] A.R. Holzwarth, Structure-function relationships and energy transfer in phycobiliprotein antennae, Physiol. Plant. 83 (1991) 518–528.
[9] L. Tian, M. Gwizdala, Ivo H.M. van Stokkum, Rob B.M. Koehorst, D. Kirilovsky, H. van Amerongen, Picosecond kinetics of light harvesting and photoprotective quenching in wild-type and mutant phycobilisomes isolated from the cyanobacterium synechocystis PCC 6803, Biophys. J. 102 (2012) 1692–1700.
[10] I.H.M. van Stokkum, M. Gwizdala, L. Tian, J.J. Snellenburg, R. van Grondelle, H. van Amerongen, R. Berera, A functional compartmental model of the Synechocystis PCC 6803 phycobilisome, Photosynth. Res. 135 (2018) 87–102.
[11] A. McGregor, M. Klartag, L. David, N. Adir, Allophycocyanin trimer stability and functionality are primarily due to polar enhanced hydrophobicity of the phycocyanobilin binding pocket, J. Mol. Biol. 384 (2008) 406–421.
[12] M. Watanabe, D.A. Semchonok, M.T. Webber-Birungi, S. Ehira, K. Kondo, R. Narikawa, M. Ohmori, E.J. Boekema, M. Ikeuchi, Attachment of phycobilisomes in an antenna–photosystem I supercomplex of cyanobacteria, Proc. Natl. Acad. Sci. 111 (2014) 2512–2517.
[13] D.J. Lundell, A.N. Glazer, Molecular architecture of a light-harvesting antenna. Structure of the 18 S core-rod subassembly of the Synechococcus 6301 phycobilisome, J. Biol. Chem. 258 (1983) 894–901.
[14] D.V. Zlenko, T.V. Galochkina, P.M. Krasilnikov, I.N. Stadnichuk, Coupled rows of PBS cores and PSII dimers in cyanobacteria: symmetry and structure, Photosynth. Res. 133 (2017) 245–260.
[15] V. Capuano, A.S. Braux, N. Tandeau de Marsac, J. Houmard, The "anchor polypeptide" of cyanobacterial phycobilisomes. Molecular characterization of the Synechococcus sp. PCC 6301 apce gene, J. Biol. Chem. 266 (1991) 7239–7247.
[16] D.J. Lundell, A.N. Glazer, Molecular architecture of a light-harvesting antenna. Core substructure in Synechococcus 6301 phycobilisomes: two new allophycocyanin and allophycocyanin B complexes, J. Biol. Chem. 258 (1983) 902–908.
[17] Y.M. Gindt, J. Zhou, D.A. Bryant, K. Sauer, Spectroscopic studies of phycobilisome subcore preparations lacking key core chromophores: assignment of excited state

energies to the Lcm, β18 and αAP-B chromophores, Biochim. Biophys. Acta 1186 (1994) 153–162.
[18] H. Liu, H. Zhang, D.M. Niedzwiedzki, M. Prado, G. He, M.L. Gross, R. E. Blankenship, Phycobilisomes supply excitations to both photosystems in a megacomplex in cyanobacteria, Science 342 (2013) 1104–1107.
[19] M. Watanabe, M. Ikeuchi, Phycobilisome: architecture of a light-harvesting supercomplex, Photosynth. Res. 116 (2013) 265–276.
[20] L.K. Anderson, F.A. Eiserling, Asymmetrical core structure in phycobilisomes of the cyanobacterium Synechocystis 6701, J. Mol. Biol. 191 (1986) 441–451.
[21] D.V. Zlenko, P.M. Krasilnikov, I.N. Stadnichuk, Structural modeling of the phycobilisome core and its association with the photosystems, Photosynth. Res. 130 (2016) 347–356.
[22] M. Watanabe, M. Ikeuchi, Phycobilisome: architecture of a light-harvesting supercomplex, Photosynth. Res. 116 (2013) 265–276.
[23] W. Reuter, C. Nickel, W. Wehrmeyer, Isolation of allophycocyanin B from Rhodella violacea results in a model of the core from hemidiscoidal phycobilisomes of rhodophyceae, FEBS Lett. 273 (1990) 155–158.
[24] K. El Bissati, E. Delphin, N. Murata, A.L. Etienne, D. Kirilovsky, Photosystem II fluorescence quenching in the cyanobacterium Synechocystis PCC 6803: involvement of two different mechanisms, Biochim. Biophys. Acta 1457 (2000) 229–242.
[25] M.G. Rakhimberdieva, I.N. Stadnichuk, I.V. Elanskaya, N.V. Karapetyan, Carotenoid-induced quenching of the phycobilisome fluorescence in photosystem II-deficient mutant of Synechocystis sp, FEBS Lett. 574 (2004) 85–88.
[26] A. Wilson, G. Ajlani, J.-M. Verbavatz, I. Vass, C.A. Kerfeld, D. Kirilovsky, A soluble carotenoid protein involved in phycobilisome-related energy dissipation in cyanobacteria, Plant Cell 18 (2006) 992–1007.
[27] M. Gwizdala, A. Wilson, D. Kirilovsky, In vitro reconstitution of the cyanobacterial photoprotective mechanism mediated by the orange carotenoid protein in synechocystis PCC 6803, Plant Cell 23 (2011) 2631–2643.
[28] A. Wilson, C. Punginelli, A. Gall, C. Bonetti, M. Alexandre, J.-M. Routaboul, C. A. Kerfeld, R. van Grondelle, B. Robert, J.T.M. Kennis, D. Kirilovsky, A photoactive carotenoid protein acting as light intensity sensor, Proc. Natl. Acad. Sci. 105 (2008) 12075–12080.
[29] Eugene G. Maksimov, Evgeny A. Shirshin, Nikolai N. Sluchanko, Dmitry V. Zlenko, Evgenia Y. Parshina, Georgy V. Tsoraev, Konstantin E. Klementiev, Gleb S. Budylin, F.-J. Schmitt, T. Friedrich, Victor V. Fadeev, Vladimir Z. Paschenko, Andrew B. Rubin, The signaling state of orange carotenoid protein, Biophys. J. 109 (2015) 595–607.
[30] N.N. Sluchanko, Y.B. Slonimskiy, E.G. Maksimov, Features of protein−protein interactions in the cyanobacterial photoprotection mechanism, Biochem. Mosc. 82 (2017) 1592–1614.
[31] M. Gwizdala, A. Wilson, D. Kirilovsky, In vitro reconstitution of the cyanobacterial photoprotective mechanism mediated by the orange carotenoid protein in synechocystis PCC 6803, Plant Cell 23 (2011) 2631–2643.
[32] A.L. Wilson, G. Ajlani, J.-M. Verbavatz, I. Vass, C.A. Kerfeld, D. Kirilovsky, A soluble carotenoid protein involved in phycobilisome-related energy dissipation in cyanobacteria, Plant Cell 18 (2006) 992–1007.
[33] D. Kirilovsky, Modulating energy arriving at photochemical reaction centers: orange carotenoid protein-related photoprotection and state transitions, Photosynth. Res. 126 (2015) 3–17.
[34] M.A. Domínguez-Martín, P.V. Sauer, H. Kirst, M. Sutter, D. Bína, B.J. Greber, E. Nogales, T. Polívka, C.A. Kerfeld, Structures of a phycobilisome in light-harvesting and photoprotected states, Nature 609 (2022) 835–845.
[35] L. Tian, I.H.M. van Stokkum, R.B.M. Koehorst, A. Jongerius, D. Kirilovsky, H. van Amerongen, Site, rate, and mechanism of photoprotective quenching in cyanobacteria, J. Am. Chem. Soc. 133 (2011) 18304–18311.
[36] H. Zhang, H. Liu, D.M. Niedzwiedzki, M. Prado, J. Jiang, M.L. Gross, R. E. Blankenship, Molecular mechanism of photoactivation and structural location of the cyanobacterial orange carotenoid protein, Biochemistry 53 (2014) 13–19.
[37] I.V. Elanskaya, D.V. Zlenko, E.P. Lukashev, N.E. Suzina, I.A. Kononova, I. N. Stadnichuk, Phycobilisomes from the mutant cyanobacterium Synechocystis sp. PCC 6803 missing chromophore domain of ApcE, Biochim. Biophys. Acta 2018 (1859) 280–291.
[38] F.I. Kuzminov, N.V. Karapetyan, M.G. Rakhimberdieva, I.V. Elanskaya, M. Y. Gorbunov, V.V. Fadeev, Investigation of OCP-triggered dissipation of excitation energy in PSI/PSII-less Synechocystis sp. PCC 6803 mutant using non-linear laser fluorimetry, Biochim. Biophys. Acta 2012 (1817) 1012–1021.
[39] I.N. Stadnichuk, M.F. Yanyushin, E.G. Maksimov, E.P. Lukashev, S. K. Zharmukhamedov, I.V. Elanskaya, V.Z. Paschenko, Site of non-photochemical quenching of the phycobilisome by orange carotenoid protein in the cyanobacterium Synechocystis sp. PCC 6803, Biochim. Biophys. Acta 2012 (1817) 1436–1445.
[40] L. Landau, On the thermodynamics of photoluminescence, J. Phys. (Moscow) 10 (1946).
[41] G.V. Tsoraev, E.A. Protasova, E.A. Klimanova, Y.L. Ryzhykau, A.I. Kuklin, Y. S. Semenov, B. Ge, W. Li, S. Qin, T. Friedrich, N.N. Sluchanko, E.G. Maksimov, Anti-stokes fluorescence excitation reveals conformational mobility of the C-phycocyanin chromophores, Struct. Dyn. 9 (2022).
[42] E.G. Maksimov, N.N. Sluchanko, Y.B. Slonimskiy, E.A. Slutskaya, A.V. Stepanov, A. M. Argentova-Stevens, E.A. Shirshin, G.V. Tsoraev, K.E. Klementiev, O. V. Slatinskaya, E.P. Lukashev, T. Friedrich, V.Z. Paschenko, A.B. Rubin, The photocycle of orange carotenoid protein conceals distinct intermediates and asynchronous changes in the carotenoid and protein components, Sci. Rep. 7 (2017) 15548.
[43] M. Golub, M. Moldenhauer, O. Matsarskaia, A. Martel, S. Grudinin, D. Soloviov, A. Kuklin, E.G. Maksimov, T. Friedrich, J. Pieper, Stages of OCP–FRP interactions in the regulation of photoprotection in cyanobacteria, part 2: small-angle neutron scattering with partial deuteration, J. Phys. Chem. B 127 (2023) 1901–1913.
[44] X. Wang, W. Li, M. Xie, F. Zhao, G. Yang, Q. Liu, S. Qin, The energy transfer dynamics in C-phycocyanin hexamer from Spirulina platensis, Chin. Sci. Bull. 63 (2018) 641–648.
[45] X. Guan, S. Qin, Z. Su, F. Zhao, B. Ge, F. Li, X. Tang, Combinational biosynthesis of a fluorescent cyanobacterial Holo-α-Phycocyanin in Escherichia coli by using one expression vector, Appl. Biochem. Biotechnol. 142 (2007) 52–59.
[46] Y. Yang, B. Ge, X. Guan, W. Zhang, S. Qin, Combinational biosynthesis of a fluorescent cyanobacterial holo-α-allophycocyanin in Escherichia coli, Biotechnol. Lett. 30 (2008) 1001–1004.
[47] W. Zhang, X. Guan, Y. Yang, B. Ge, H. Chen, F. Li, S. Qin, Biosynthesis of fluorescent allophycocyanin α-subunits by autocatalysis in Escherichia coli, Biotechnol. Appl. Biochem. 52 (2009) 135–140.
[48] D.V. Zlenko, I.V. Elanskaya, E.P. Lukashev, Y.V. Bolychevtseva, N.E. Suzina, E. S. Pojidaeva, I.A. Kononova, A.V. Loktyushkin, I.N. Stadnichuk, Role of the PB-loop in ApcE and phycobilisome core function in cyanobacterium Synechocystis sp. PCC 6803, Biochim. Biophys. Acta 2019 (1860) 155–166.
[49] L. David, M. Prado, A.A. Arteni, D.A. Elmlund, R.E. Blankenship, N. Adir, Structural studies show energy transfer within stabilized phycobilisomes independent of the mode of rod–core assembly, Biochim. Biophys. Acta 1837 (2014) 385–395.
[50] P. Bevington, D.K. Robinson, Data Reduction and Error Analysis for the Physical Sciences, Place Published, McGraw-Hill Education, 2003.
[51] D. Harris, O. Tal, D. Jallet, A. Wilson, D. Kirilovsky, N. Adir, Orange carotenoid protein burrows into the phycobilisome to provide photoprotection, Proc. Natl. Acad. Sci. U. S. A. 113 (2016) E1655–E1662.